Available online at www.sciencedirect.com

ScienceDirect

Procedia CIRP 92 (2020) 181–186

www.elsevier.com/locate/procedia

16th CIRP Conference on Computer Aided Tolerancing (CIRP CAT 2020)

Exploring Registration of Optical, CMM and XCT for Verification of Supplemental Surfaces to Define AM Lattices: Application to Cylindrical and Spherical Surfaces

Maxwell Praniewicz[a]*, Jason Fox[b], Gaurav Ameta[c], Felix Kim[b], Paul Witherell[b], Christopher Saldana[a]

[a] George W. Woodruff School of Mechanical Engineering, Georgia Institute of Technology, 801 Ferst Drive, Atlanta, Georgia 30332
[b] National Institute of Standards and Technology , Gaithersburg, MD 20899
[c] Siemens Corporate Research, Princeton, NJ 08540

* Corresponding author. *E-mail address:* max.praniewicz@gatech.edu

Abstract

The use of lattice structures produced using additive manufacturing (AM) is of great interest to the aerospace and medical industries because of their potential for strength/weight optimization. However, their use is often limited due to challenges in qualification. Recent standards proposed for the definition and verification of lattice structures created using AM attempt to address these gaps. In this work, a lattice component is designed using a repeated unit cell and theoretical supplemental surfaces (TSS), brought forth in ASME Y14.46, are used to define the bounding geometry of the component. Two planes and a sphere are used to define a datum hierarchy that will be used to qualify the component. A measurand is defined by a spherical TSS and is later used to evaluate the quality of datum registration. The component is produced using a laser powder bed fusion process and then measured using focus variation microscopy, X-Ray computed tomography, and a coordinate measuring machine (CMM). The three data sources are then registered using a refined sampling registration based on the CMM points. The effect of CMM data acquisition strategy on the quality of the registration is then examined. Results show that CMM planning based on optical measurements of the component, as opposed to the designed geometry, show significant improvement in the quality of registration. This work highlights the importance of sampling location in tactile measurements of components produced using additive manufacturing and recommends that definition of inspection locations/methods be integrated into the design cycle of AM parts.

Keywords: Qualification; Tolerancing; Lattices; Additive Manufacturing

1. Introduction

Additive manufacturing (AM) processes allow for the creation of features such as complex mold cooling channels, embedded components/electronics, topology optimized structures, internal features, and lattice structures. These possibilities have prompted an entire field of research specifically focused on design for AM [1]. While the design possibilities of AM are numerous, their implementation in production has been limited by the inability to adequately qualify the manufactured components. The geometric intricacy of parts and the complexity of the manufacturing process itself makes the definition and validation of these components challenging. This creates greater requirements from product definition data in order to properly convey design intent [2, 3]. Recent activities within the standards community have worked to further develop the product definition guidelines for AM. ISO/ASTM 52910-18 has put forth detailed recommendations on design for AM, specifically highlighting challenges traditional designers may encounter in this emerging process [4]. ASME Y14.46-17 [5] has recently been released to supplement ASME Y14.5-2009

10.1016/j.procir.2020.05.182

[6] and ISO 1101:2017 [7] to define features specific to parts planned for additive manufacturing. These additions include control frames for the definition of build orientation, functionally graded materials, and support structures. This standard also put forth the methodology for controlling the boundary of lattice geometries using a theoretical supplemental surface (TSS) or theoretical supplemental geometry (TSG). Lattice structures are often comprised of a unit cell which is then repeated in an array pattern to form an object or volume within a part. In some lattice geometries, the boundary of this repeated array is trimmed by an additionally defined surface, which may divide the unit cells. Examples of these geometries can be found in heat exchangers, structural components, and medical implants [8-10].

With these new definitions, structures can now be compared to their defining theoretical boundaries. However, the qualification of additively manufactured components is non-trivial and has developed its own research community [11]. The use of X-ray Computed Tomography (XCT) and optical metrology, such as focus variation microscopy (FVM) to qualify lattice structures has grown significantly in popularity. XCT has been used to detect porosity, lattice quality, and inspect internal features [12-14]. However, the use of XCT as a metrological technique is limited, as determining measurement uncertainty is non-trivial [15]. Optical measurements have been used to resolve the topology of AM surface to a high level of detail [16]; however, optical measurements are limited by line of sight and can often be very time consuming due to the small window size of an individual field-of-view. While Coordinate Measuring Machines (CMMs) have often been the preferred qualification method for components produced via traditional processes due to their high accuracy and repeatability, they are less favorable for the measurement of AM components. This is due to mechanical filtering caused by the varying surface texture produced by the AM process [17]. Thus, it would be advantageous to utilize the benefits from all qualification techniques to "fully qualify" a component. Other works have investigated the combination of multiple measurement methods for this purpose [18, 19].

The usage of the TSS to define and qualify lattice structures manufactured using AM has been limited. Ameta et al. used the TSS to define a lattice, but only evaluated form with FVM [20]. Praniewicz et al. defined an AM component using solid datum features and a lattice measurand defined by a TSS [21]. Measurement data from XCT and CMM were registered to the nominal geometry and a refined sampling technique was presented to improve the quality of the registration process. That work also remarked on the importance of consistent sampling locations in the registration of AM measurement data. However, previous work did not examine the use of a TSS to define a datum on a lattice, which is crucial for the evaluation of complex lattice components.

In this work, measurement data from three sources (CMM, XCT, FVM) are used to evaluate a lattice defined by TSG. A lattice object is designed and presented using TSG. The measurement methodology for each technique is described. The data sets are then registered using a refined region sampling and compared to the as-designed geometry. The effect of path planning methodology on CMM is evaluated using programed positions from both the CAD and data from non-contact inspection. A discussion on the evaluation of TSG using contact inspection is then presented.

2. Methodology

2.1. Component Geometry

The geometry constructed for this study was created using a repeated unit cell measuring 1.66 mm per side, shown in Figure 1 (a). The unit cell was first patterned to create a larger prismatic geometry, represented as the dotted line in Figure 1 (b). The lattice was formed by the intersection of the patterned lattice and the volume defined by several TSSs, shown as the solid lines in Figure 1 (b). The final lattice geometry can be seen in Figure 1 (c).

The bounding TSS volume was defined using the drawing in Figure 1 (d). A cylindrical TSS with a radius of 8.89 mm was designated as datum A and positioned offset from the corner of the prismatic geometry by 0.511 mm and 0.154 mm in the X+ and Z- directions, respectively, with the axis of the cylinder parallel to the Y axis. Datum B was designated as the planar surface facing the Y- direction. Datum C was designated as the planar surface facing the X- direction. A spherical TSS was designed with the center point translated 4.074 mm along the axis of the cylindrical TSS and a radius equal to the cylinder radius. This surface was assigned a profile tolerance and will be evaluated as the measurand in this study.

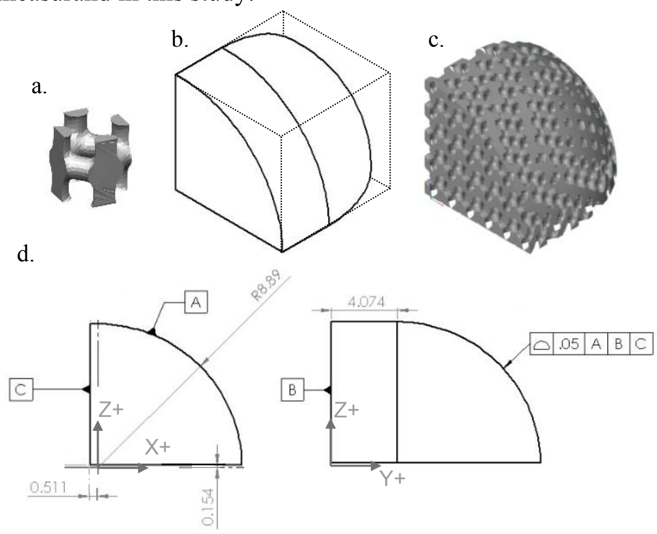

Figure 1: Unit cell (a), Prismatic and TSS volume (b), Final lattice (c), Dimensioned TSS volume dimensioned in mm (d)

The designed component was then manufactured on an EOS M290 from nickel superalloy 625 using the manufacturer designated parameters for a 0.04 mm layer height. The component was oriented within the machine volume such that the build direction coincided with the Z+ axis of the part.

2.2. Measurement Methodology

The optical FVM measurement process was performed using an Alicona InfiniteFocus G5 with Real3D rotation unit. The lattice structure was affixed to a platform and held using the rotation unit. This allowed for multiple measurements with rotation about the X+ and Y+ axes of the part, which were aligned to the microscope axes by visual inspection. Individual measurements were performed at rotations listed in Table 1. All measurements were performed using a 5x objective having a 0.15 mm numeric aperture. This created a 1.76 µm point spacing for each individual measurement. Note that the system has a 23.5 mm working distance with the 5x objective, allowing for a large vertical range of the part to be measured at each position. The individual measurements were stitched using the system's built in software to create a true three-dimensional dataset and exported from the system as a stereolithography file (STL).

Table 1: FVM measurement rotation Settings

Measurement	1	2	3	4	5
Rotation about X+	0°	-15°	30°	0°	0°
Rotation about Y+	0°	0°	0°	30°	-30°

An industrial XCT system with a 225 kV source and a flat panel detector was used for the XCT measurements. The scanning parameters are shown in Table 2. Vendor-supplied software was used to perform beam hardening correction and Feldkamp-Davis-Kress (FDK) algorithm-based reconstruction [22]. Beam hardening correction was applied to improve uniformity of image intensity. The XCT data was imported into VGStudioMax 3.1 [23] for surface determination and for exporting a surface mesh. Iterative sub-voxel surface determination process was applied to a global threshold-based initial surface [24]. A four voxel search distance was applied. Based on the determined surface, a surface mesh was created.

Table 2: XCT scanning parameters

Parameter	Values
Voltage	220 kV
Current	100 µA
Target material	Tungsten
Filter (material; thickness)	Cu; 4.06 mm
Source-to-detector distance	530.67 mm
Source-to-object distance	83.29 mm
Magnification	6.37
Flat panel detector pixel pitch	127 µm
Effective voxel size	19.94 µm
Number of projections	1200 µm
Frames per projection	1
Frame rate	1.5 frames/s

The component was then inspected using a Zeiss Micura CMM, which has calibrated maximum permissible error of length measurement (E0,MPE) of (0.8 + L/400) µm according to ISO 10360-2:2009 [25]. The component was then manually registered within the machine coordinate system by manually probing points on the datum surfaces using an 8 mm diameter stylus. The automated measurement routine then probed individual points on all TSS-defined surfaces using a 1.5 mm diameter stylus and a 20 mN probing force. The automated measurement routine was defined using two different methods.

The first method (method 1) utilized the as-designed geometry to inform the probing point locations. Individual points were selected on the exterior of the lattice with the largest surface area (such as a node location) in order to maximize the area of potential contact. The number of probing points chosen for each surface is displayed in Table 3.

Table 3: Probed points per surface, CAD based inspection

	Datum A	Datum B	Datum C	Measurand
Number of Points	20	18	23	58

The second method (method 2) utilized surface data from non-contact inspection to inform the location of probing points. In this method, the probing locations were chosen based on the surface data from FVM inspection. Points were then chosen where the surface data intersected the closed body. These points and a surface model were then imported into the CMM software for path planning.

2.3. Data registration and analysis

In order to evaluate the acquired data, all three data sets were registered within the same part coordinate system determined by the CMM measurements. The FVM and XCT data were initially registered to the defined datum scheme by manually selecting portions of the surface data. First, a cylinder was fit to the primary datum surface. Then, data from the secondary datum was projected onto the cylinder axis and then average point was chosen to constrain translation along the axis. Finally, data from the tertiary datum was used to constrain rotation about the cylinder axis. Once all data sets were initially registered, they were imported into MATLAB and were registered once again based on a refined region sampling using the CMM points, similar to ref. [21]. In this registration process, the point selection for datum fitting would change for the FVM and XCT data between the two methodologies due to changes in the CMM point locations. After all data sets were registered, a comparison between each data set and the design is performed and the measurand was evaluated using a least-squares fit to the sampled data. All least squares algorithms were constructed based on recommendations from the NIST algorithm testing service [26] and were verified for accuracy using the reference datasets [27].

3. Results

Figure 2 shows the individual data sets captured from the measurement methods and the surfaces fit to the component data. As one can see, there are significant differences in the quantity of data for each method. While XCT in total contains more data of the full part, the FVM provides the greatest detail on the exterior surfaces. In order to fit datum

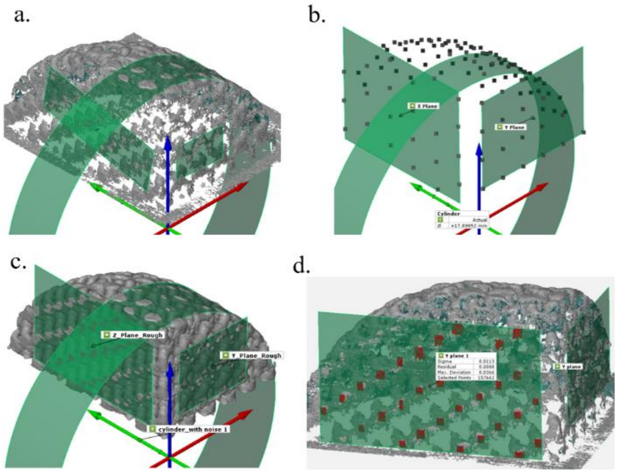

Figure 2: Individual measurement data and created fit surfaces: (a) FVM (b) CMM (c) XCT. (d).Example of manually selected surfaces for fitting

surfaces, groups of discrete points corresponding to each datum must be extracted from the data set. This is relatively easy for the CMM set, as these groups can easily be extracted because of relatively sparse data (see Figure 2 (b)). However, this is not a trivial task for the FVM and XCT data. Figure 2 (d) shows an example of this data extraction, where the points in red were used to fit a plane to datum C of the FVM data set.

Figure 3 shows the deviation from CAD for both the FVM and XCT data after the registration is complete for method 1. As one can see, there is a significant discrepancy between the CAD geometry and the manufactured component, with majority of points deviating more than 0.1 mm. This is inconsistent with the fit cylinders for both data sets, which indicate that the component was manufactured larger than the initial design. A large difference of 0.30 mm and 0.27 mm was also observed between CMM and the XCT and FVM respectively. Upon examination, it was observed that most of the points used in the refined region registration were not consistently located at their as-designed position. The non-contact based CMM inspection (method 2) was inspected for similar result.

Figure 4 shows the process of creating geometry for method 2 path planning from FVM data. First, geometry was fit to each group using least squares. A volume was then formed by determining the Boolean union of the cylindrical and spherical regions. This volume was then trimmed by removing any material exterior the fit planes. Individual probing points were manually selected on the exterior nodes of the FVM mesh. These points were then transferred to the volume as the intersection of different surface patches and were assigned as probing points in the CMM software.

Figure 5 shows the deviation from CAD for the FVM and XCT data for the non-contact-based measurements (method 2). The deviation map for the registered data shows a greater consistency in the refined region registration. Both data sets show that the component was manufactured oversized, with the majority of data points showing positive deviation, but the magnitude is much less than method 1. One can also see that that the spherical measurand does not conform to the surface profile tolerance defined by the TSS.

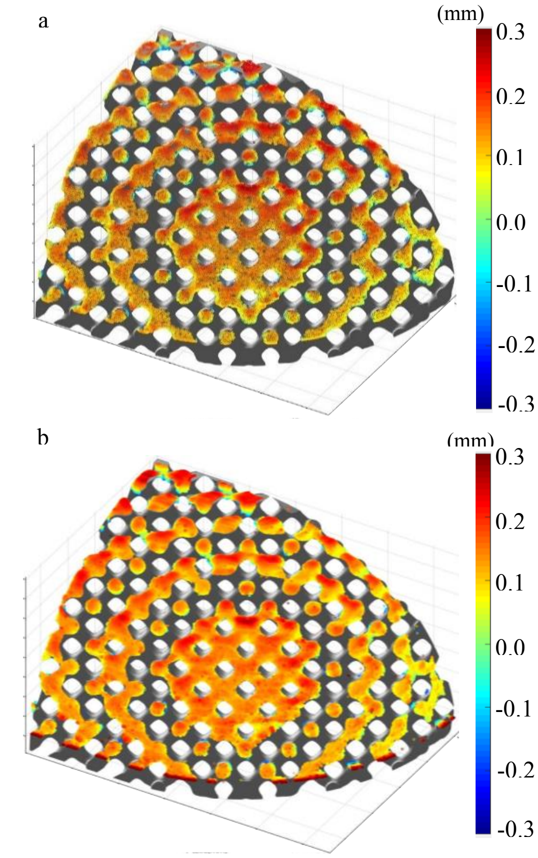

Figure 3: Measurement deviation from CAD, method 1: (a) XCT (b) FVM

Table 4 shows the fit measurand results from method 2. These show, once again, that the component is larger than intended, though the values appear to change as a result of sampling location. The CMM probe contacts the exterior of the component, while the two noncontact measurement methods can extend into the lattice. Thus, it is expected that the CMM measurement is larger than the FVM and XCT.

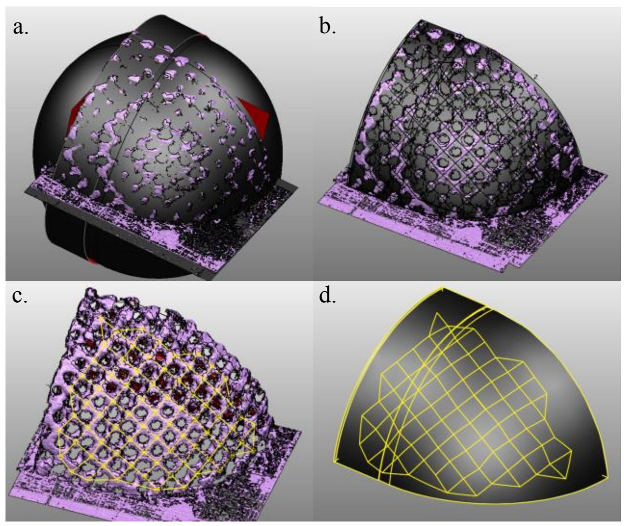

Figure 4: Construction of non-contact-based geometry for CMM path planning: (a) Geometry fitting (b) Volume creation (c) Point selection (d) Point transfer

Table 4: Measurement results from method 2

	Sphere Diameter (mm)	X Position (mm)	Y Position (mm)	Z Position (mm)
Designed	17.780	0.0	4.074	0.0
XCT	17.98	0.00	3.99	0.00
FVM	17.97	0.01	4.00	0.00
CMM	18.055	0.008	4.002	0.002

Table 5 shows the range in the parameters of the fit measurand between the two CMM inspection methods. The range in diameters over the three measurement methods has been reduced by 0.21 mm using method 2. While this reduction is only 2% of the nominal diameter, it is significant compared to the stated measurement uncertainty of the three measurement methods. The range of the position of the fit sphere is also reduced along all three axes for the non-contact-based measurements.

Table 5: Measurand parameters for both methods

	Diameter Range (mm)	X Range (mm)	Y Range (mm)	Z Range (mm)
CAD based Alignment	0.30	0.02	0.05	0.02
Non-contact Alignment	0.09	0.01	0.04	0.01

4. Discussion

In the presented results, the FVM and XCT sets evaluated were not changed between the two CMM measurement methods. The differences in measurement result from changes in point sampling during the registration process. Figure 6 shows the variation in topology between the CAD and non-contact measurements. As described in the results section, the topology of the surface is seen to fluctuate throughout a region defined by a given TSS. Thus, variation in the location of inspection points can result in changes in

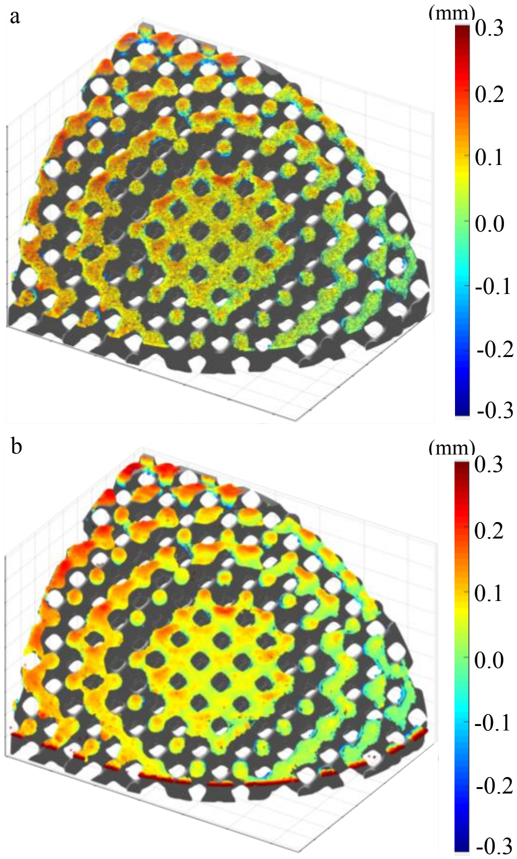

Figure 5: Measurement deviation from CAD, method 2: (a) XCT (b) FVM

form measurement. While the CAD model in Figure 6 (a) shows the exterior of the lattice as one trimmed by a continuous spherical surface, this is not clear in the inspection of the as-manufactured component. The CAD model also displays a sharp transition between the exterior of the lattice and the interior struts. This distinction between the exterior (which is defined by the TSS) and the interior of the lattice structure is hard to discern in the inspection data, making it difficult to determine appropriate sampling locations to evaluate form.

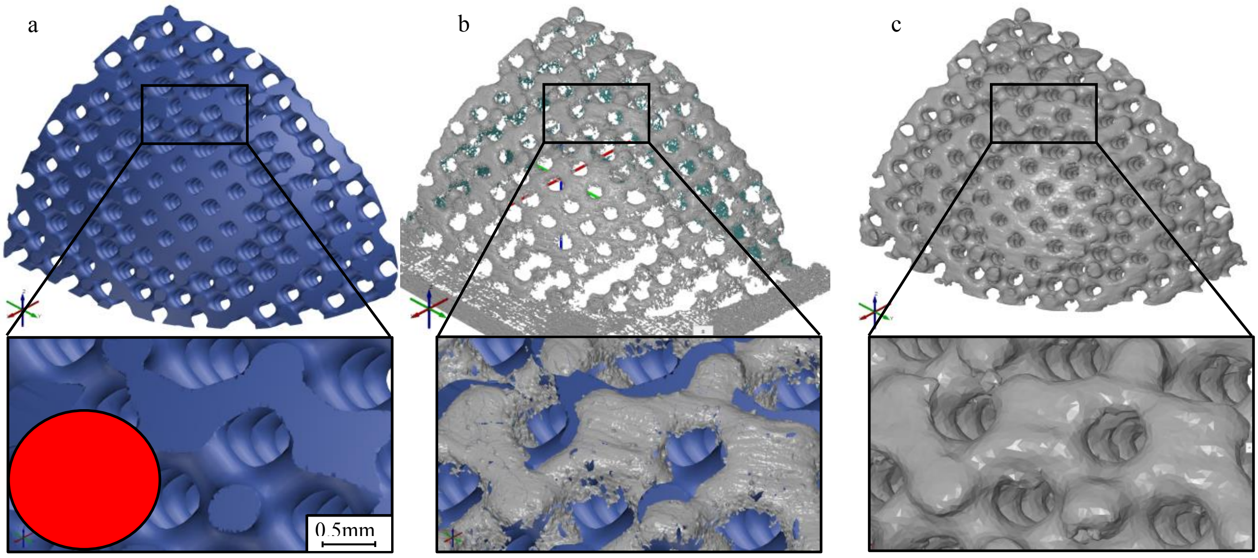

Figure 6: Display of differences in surface topology: (a) CAD model with CMM probe shown in red for scale (b) FVM inspection data (gray) overlaid on CAD model (blue) (c) XCT inspection data

In order to evaluate form on a lattice defined by a TSS, additional specification must be provided by the designer to define sampling cutoffs. These specifications could involve designation of sampling areas utilizing prior knowledge of the manufacturing process limits. Development of these specifications would not only aid in the tolerancing and qualification of AM lattice components, but would also aid the entire GPS community, as data extraction and filtration are two major research efforts [28]. It is recommended that provisions for sampling specifications be incorporated into future revisions of the respective standards. Investigation of sampling techniques will be the subject of future research.

Conclusion

In this work, a lattice structure was designed using theoretical supplemental surfaces as defined in ASME Y14.46. The component was then produced using an additive manufacturing process and measured using focus variation microscopy, XCT, and a CMM. The measurements were registered using a refined sampling registration based on the CMM points. The effect of CMM data acquisition strategy on the quality of the registration was examined. Results showed that CMM planning based on non-contact measurements, as opposed to the designed geometry, significantly improves the quality of registration. An additional discussion was presented on the importance of data sampling in the evaluation of complex AM components. Future work will focus on defining and evaluating sampling techniques for measuring form on open cell lattice structures.

Acknowledgements

M. Praniewicz would like to acknowledge fellowship support from the National Physical Sciences Consortium (NPSC) and the National Institute of Standards and Technology (NIST).

Disclaimer

Certain commercial entities, equipment, or materials may be identified in this document to describe an experimental procedure or concept adequately. Such identification is not intended to imply recommendation or endorsement by the National Institute of Standards and Technology, nor is it intended to imply that the entities, materials, or equipment are necessarily the best available for the purpose.

References

[1]Thompson, M. K. *et al.*, "Design for Additive Manufacturing: Trends, opportunities, considerations, and constraints," (in English), *Cirp Annals-Manufacturing Technology,* vol. 65, no. 2, pp. 737-760, 2016.
[2]Ameta, G., R. Lipman, S. Moylan, and P. Witherell, "Investigating the Role of Geometric Dimensioning and Tolerancing in Additive Manufacturing," (in English), *Journal of Mechanical Design,* vol. 137, no. 11, p. 111401, Nov 2015.
[3]Witherell, P., J. Herron, and G. Ameta, "Towards Annotations and Product Definitions for Additive Manufacturing," (in English), *14th Cirp Cat 2016 - Cirp Conference on Computer Aided Tolerancing,* vol. 43, pp. 339-344, 2016.
[4]*ASTM ISO/ASTM52910-18 Additive manufacturing — Design — Requirements, guidelines and recommendations*, 2018.
[5]*ASME Y14.46-2017 Product Definition for Additive Manufacturing*, 2017.
[6]*Y14.5-2009: Dimensioning and Tolerancing*, 2018.
[7]*ISO 1101:2017 Geometrical product specifications (GPS) — Geometrical tolerancing — Tolerances of form, orientation, location and run-out*, 2017-02.
[8]Brooks, H. and K. Brigden, "Design of conformal cooling layers with self-supporting lattices for additively manufactured tooling," *Additive Manufacturing,* vol. 11, pp. 16-22, 2016.
[9]Murr, L. E., S. M. Gaytan, E. Martinez, F. Medina, and R. B. Wicker, "Next generation orthopaedic implants by additive manufacturing using electron beam melting," *International journal of biomaterials,* vol. 2012, 2012.
[10]Zheng, X. *et al.*, "Ultralight, ultrastiff mechanical metamaterials," *Science,* vol. 344, no. 6190, pp. 1373-7, Jun 20 2014.
[11]Leach, R., D. Bourell, S. Carmignato, A. Donmez, N. Senin, and W. Dewulf, "Geometrical metrology for metal additive manufacturing," *CIRP Annals,* 2019.
[12]Biswal, R. *et al.*, "Interrupted fatigue testing with periodic tomography to monitor porosity defects in wire+ arc additive manufactured Ti-6Al-4V," *Additive Manufacturing,* 2019.
[13]Dressler, A. D., E. W. Jost, J. C. Miers, D. G. Moore, C. C. Seepersad, and B. L. Boyce, "Heterogeneities Dominate Mechanical Performance of Additively Manufactured Metal Lattice Struts," *Additive Manufacturing,* 2019.
[14]Kim, F. H., H. Villarraga-Gómez, and S. P. Moylan, "Inspection of embedded internal features in additively manufactured metal parts using metrological x-ray computed tomography," in *2016 Summer Topical Meeting: Dimensional Accuracy and Surface Finish in Additive Manufacturing*, 2016.
[15]Ferrucci, M., "Towards traceability of CT dimensional measurements," in *Industrial X-Ray Computed Tomography*: Springer, 2018, pp. 229-266.
[16]Townsend, A., N. Senin, L. Blunt, R. K. Leach, and J. S. Taylor, "Surface texture metrology for metal additive manufacturing: a review," (in English), *Precision Engineering-Journal of the International Societies for Precision Engineering and Nanotechnology,* vol. 46, pp. 34-47, Oct 2016.
[17]Carmignato, S. and E. Savio, "Traceable volume measurements using coordinate measuring systems," (in English), *Cirp Annals-Manufacturing Technology,* vol. 60, no. 1, pp. 519-522, 2011.
[18]Zanini, F., E. Sbettega, M. Sorgato, and S. Carmignato, "New approach for verifying the accuracy of X-ray computed tomography measurements of surface topographies in additively manufactured metal parts," *Journal of Nondestructive Evaluation,* vol. 38, no. 1, p. 12, 2019.
[19]Fox, J. C., F. Kim, Z. Reese, and C. Evans, "Complementary use of optical metrology and X-ray computed tomography for surface finish and defect detection in laser powder bed fusion additive manufacturing," in *2018 ASPE and euspen Summer Topical Meeting-Advancing Precision in Additive Manufacturing*, 2018, vol. 69.
[20]Ameta, G., J. Fox, and P. Witherell, "Tolerancing and Verification of Additive Manufactured Lattice with Supplemental Surfaces," *Procedia CIRP,* vol. 75, pp. 69-74, 2018.
[21]Praniewicz, M., J. Fox, G. Ameta, and C. Saldana, "Data registration for multi-method qualification of additive manufactured components (Under Review)," *Additive Manufacturing,* 2019.
[22]Feldkamp, L. A., L. C. Davis, and J. W. Kress, "Practical Cone-Beam Algorithm," (in English), *Journal of the Optical Society of America a-Optics Image Science and Vision,* vol. 1, no. 6, pp. 612-619, 1984.
[23]Volume_Graphics_GmbH, " VGStudioMax 3.1."
[24]Reinhart, C., "Industrial computer tomography–a universal inspection tool," in *17th world conference on nondestructive testing*, 2008, pp. 25-28: Citeseer.
[25]*ISO 10360-2:2009 Geometrical product specifications (GPS) — Acceptance and reverification,tests for coordinate measuring machines,(CMM) —Part 2: CMMs used for measuring linear dimensions*, 2009.
[26]Shakarji, C. M., "Least-Squares Fitting Algorithms of the NIST Algorithm Testing System," *J Res Natl Inst Stand Technol,* vol. 103, no. 6, pp. 633-641, Nov-Dec 1998.
[27]"nist-l2-reference-pairs," ed. https://www.nist.gov/pml/sensor-science/dimensional-metrology/algorithm-testing: National Institute of Standards and Technology 2009.
[28]Morse, E. P., C. M. Shakarji, and V. Srinivasan, "A Brief Analysis of Recent ISO Tolerancing Standards and Their Potential Impact on Digitization of Manufacturing," *Procedia CIRP,* vol. 75, pp. 11-18, 2018.